

This paper was published in the 1999 SPIE Conference Proceedings and is made available as an electronic reprint with permission of SPIE. Single print or electronic copies for personal use only are allowed. Systematic or multiple reproduction, or distribution to multiple locations through an electronic listserver or other electronic means, or duplication of any material in this paper for a fee or for commercial purposes is prohibited. By choosing to view or print this document, you agree to all the provisions of the copyright law protecting it.

Composite ultrasound transducer arrays for operation above 20 MHz

Timothy Ritter, K.Kirk Shung, Xuecang Geng, Pat Lopath, Richard Tutwiler, and Thomas Shrout

NIH Resource Center for Medical Ultrasonic Transducer Technology
Penn State University
205 Hallowell Building
University Park, PA 16802

ABSTRACT

Methods for fabricating and modeling high frequency 2-2 composites and arrays are presented. The composites are suitable for arrays and small aperture single element devices operating above 20 MHz. Coupling coefficients above 0.65 and lateral mode frequencies near 60 MHz were achieved with this composite. Backing and matching materials were prepared to provide up to 70% bandwidth and coaxial cable was used to impedance match the elements to a 50 ohm source. A TPX lens was fabricated and bonded to the face to provide focusing in the elevation direction. Three prototype 4 element 30 MHz linear arrays were designed and built. The designs were analyzed in a time domain finite element analysis program and excellent agreement between theory and experiment was achieved.

Keywords: transducers, piezoelectric composites, ultrasound arrays, high frequency arrays, finite element analysis

1. INTRODUCTION

Ultrasonic imaging applications are being driven to higher and higher frequencies. Very high frequency ultrasonic imaging systems, critical for improved diagnostic applications in dermatology and ophthalmology, await the development of arrays operating above 20 MHz. These high frequency arrays require small spatial scales ($<10\ \mu\text{m}$) which cannot be achieved using conventional fabrication techniques. Novel fabrication methods and innovative materials are therefore required.

Prototype arrays developed in this frequency range include a pair of 20 MHz PZT arrays [1][2], a 100 MHz array incorporating a sapphire lens and thin film ZnO [3], and a piezoelectric polymer array with built-in transmit and receive circuitry [4]. In addition, O'Donnell et al described the operation of a 20 MHz phased array imaging system for catheter use [5][6].

Linear arrays, which typically do not use beam-steering, can tolerate a much larger element pitch than phased arrays. It is therefore practical to focus first on the development of linear arrays with 1λ to 2λ pitch. Although integrating the array with the electronics offers advantages, a more conventional and flexible approach of coupling the array elements to a 50 ohm imaging system has been adopted. Broad bandwidth (minimum of 40%) is desired, both to suppress grating lobes and to improve the axial resolution. Crosstalk levels of near -30dB are considered acceptable for a linear array not incorporating Doppler. Finally, mild elevational focusing is desired for improved resolution in the elevation direction.

2. COMPOSITE FABRICATION

PZT “strip” vibrators (length \gg width or height) with free boundary conditions require a width to height ratio of less than approximately 0.6 for proper pulse performance. For 30 MHz operation each PZT strip must therefore measure approximately $30\mu\text{m}$ wide by $50\mu\text{m}$ in height. For a 2-2 composite comprised of interleaved polymer and ceramic strips, optimized operation requires that the spatial scale of all constituents be much less than a wavelength. For example, the epoxy between each ceramic must be less than $10\mu\text{m}$ in order to push spurious lateral resonances above the passband of a 30 MHz array. Conventional dice and fill technology cannot presently be used to manufacture this structure. An alternative fabrication technique is to stack ceramic and polymer layers to form a block of composite material, then slice sections from this block. Variants of this technique have been proposed previously for arrays operating above 10 MHz[7]. The difficulty is in controlling the ceramic and polymer dimensions. A solution to this problem is described next.

Fine grain PZT-5H equivalent material (TRS 600, TRS Ceramics, State College, PA) was lapped to a thickness of $33\mu\text{m}$ using a precision lapping process. Numerous plates of this material were stacked and bonded together using Epo-Tek 301-2 epoxy (Epoxy Technology, Billerica, MA). The plate to plate spacing was controlled by incorporating polystyrene spheres into the bonding epoxy. These spheres (#PS06N, Bangs Laboratories, Fishers, IN) possessed a nominal diameter of $6.20\mu\text{m}$, with a standard deviation of only $0.09\mu\text{m}$. The spheres were incorporated into the epoxy at a volume fraction of 5%. Plates of $5\text{mm}\times 5\text{mm}$ ceramic and a consistent amount of loaded epoxy were stacked in an alternating fashion. The stack was constrained from lateral motion and light, uniform pressure was applied during the room temperature overnight cure. Thin sections of this stack were diced from the block, lapped to a thickness of $62\mu\text{m}$, electroded with 4000\AA of Au over a thin Cr layer, and poled at 2000V/mm and 50°C .

Analysis of the performance was encouraging and the results are listed in Table I. Note the small standard deviation in kerf, indicating this technique can provide a controlled polymer width to within $0.3\mu\text{m}$. The observed value for the lateral mode frequency corresponds closely to the d_{31} vibration of the ceramic plate, as expected for a 2-2 composite with a volume fraction exceeding 75% [8]. A theoretical investigation of the composite performance showed excellent agreement with these experimental results. The theoretical predictions were based on a dynamic model of guided wave propagation in the composite plate [8]. Table II below lists the theoretical results. Using this model a dispersion curve predicting resonant frequencies over a range of thicknesses was obtained.

Table I – Measured 2-2 composite properties

Kerf width	$7.7\mu\text{m}$
Standard deviation of kerf	$0.3\mu\text{m}$
Ceramic width	$33.5\mu\text{m}$
Standard deviation of ceramic	$0.5\mu\text{m}$
Dielectric constant, $\epsilon_{33}^S/\epsilon_0$	1100
Thickness velocity at F_p	4050 m/s
1 st lateral mode frequency	58.8 MHz
Coupling coefficient k_t	0.67

F_p is the parallel resonance frequency

Table II – Predicted 2-2 composite properties

Thickness velocity at F_p	4108 m/s
1 st lateral mode frequency	58.5 MHz
Coupling coefficient k_t	.71

F_p is the parallel resonance frequency

Although developed for high frequency arrays, this composite fabrication technique may be adapted to single element transducers. A wide diversity of ceramics, polymers, and particles can be used to achieve desired properties. In addition, nonuniform structures may be readily produced for suppression of lateral resonances resulting from spatial periodicity.

3. PASSIVE MATERIALS

Although the piezoelectric composite is the heart of an array transducer, backing, matching, and lens materials are needed to increase device sensitivity and bandwidth and provide focusing. A brief list of the tested materials and their properties is given in reference [11]. Materials were prepared in an effort to approximately match the impedances determined from one-dimensional modeling. A conductive epoxy backing material (E-Solder 3022, Von Roll Isola, Inc, New Haven, CT) was selected with sufficient attenuation to eliminate backing echoes over a round trip path length of 4mm (twice the backing height). The longitudinal acoustic impedance of this material was 5.5 Mrayls at 30 MHz. This same material was

centrifuged to provide a higher acoustic impedance (5.9 Mrayls) and used as the first matching layer in a dual matching layer design.

Finding a suitable lens material proved challenging. Requirements included a longitudinal velocity significantly different from tissue and a longitudinal impedance close to tissue. TPX (Mitsui Plastics, Inc., White Plains, NY) met these requirements with an impedance of 1.8 Mrayls and a longitudinal velocity of 2170 m/s. Since this velocity is greater than the ultrasound velocity in water a concave lens design was required. This is in contrast to a silicone lens material which typically requires a convex design because of an intrinsically low longitudinal sound velocity. The convex geometry may be preferred clinically since it is easily coupled to the human body, but the high attenuation in silicone materials results in very low device sensitivity. The concave TPX design was preferred acoustically because of the inherently low attenuation. In addition, any attenuation in the lens may serve to favorably apodize the beam [9].

4. ELECTRICAL MATCHING

In addition to acoustic impedance matching, electrical impedance matching was addressed. The electrical impedance of the elements in the 30 MHz array was over 100 ohms. In order to match these devices to a 50 ohm system a transformer was desired. For this array excellent results were achieved using the coaxial cable connecting each element to the system. Using transmission line theory, an optimum length of low capacitance micro-coax from Precision Interconnect (Portland, OR) was selected to transform the impedance and tune out reactive components. In addition, the coax served to increase bandwidth and “fine tune” the center frequency. This technique is well suited to devices in the frequency range of 20 to 60 MHz where the length of the coax will vary from approximately 3 m to 1 m, respectively.

The impedance transformation achieved with coaxial cable was analyzed using well known transmission line equations. The first step in quantifying this transformation was to characterize the impedance (Z_0) and propagation constant (\mathbf{g}) of the coaxial cable. This was accomplished using an HP4194 impedance analyzer and the expression for the impedance transformation from a length x of coax [12]:

$$Z_x = Z_o \frac{(Z_{load} + Z_o \mathbf{Tanh}(\mathbf{g}x))}{(Z_o + Z_{load} \mathbf{Tanh}(\mathbf{g}x))} \quad (1)$$

where Z_{load} represents the load at the end of the coax and Z_x is the transformed impedance measured by the impedance analyzer. The values of Z_x for short circuit and open circuit values of Z_{load} were measured at 30 MHz and equation (1) was used to solve for \mathbf{g} and Z_o . The distributed network representation of a transmission line then resulted in the following expressions:

$$\mathbf{g} = \sqrt{(r + j\omega l)(g + j\omega c)} \quad (2)$$

$$Z_o = \sqrt{\frac{(r + j\omega l)}{(g + j\omega c)}} \quad (3)$$

The quantities $r, l, g,$ and c are the per unit length values of series resistance, series inductance, shunt conductance, and shunt capacitance, while ω is the frequency in radians per second. The propagation constant \mathbf{g} was then analyzed in terms of the real part (a or attenuation) and imaginary part (b or phase constant). The phase constant was used to obtain the velocity of propagation from the relationship:

$$c = \frac{\omega}{b} \quad (4)$$

The coax selected for this array was fully characterized using the technique described above and the results are listed in table III below. The characteristic impedance of the coax lies between the impedance values of an array element (150 to 200

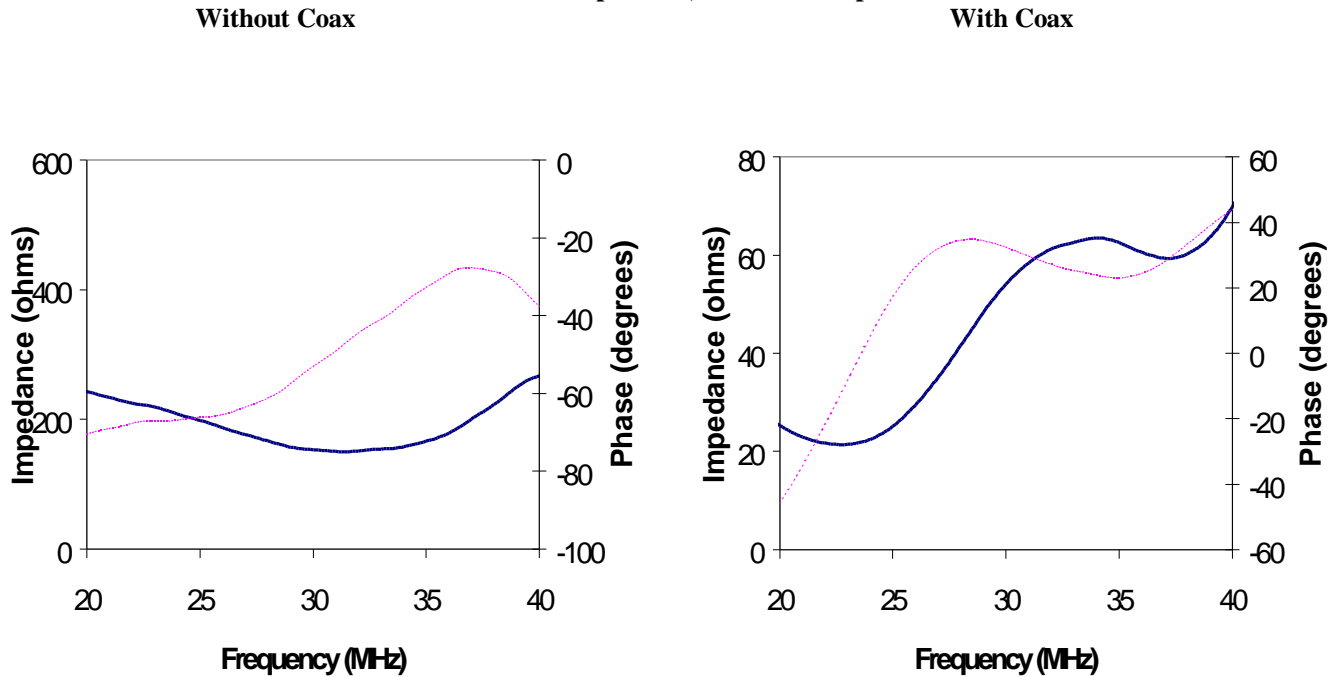
ohms) and the system (50 ohms). It was therefore possible to broaden the bandwidth of the element using this coax. Ideally, the impedance of the coax should be optimized for the array impedance.

Table III – Coax properties measured at 30 MHz

Characteristic impedance Z_0	85 - 5.2i ohms
Propagation constant γ	0.051 + 0.78i
Propagation velocity	2.4×10^8 m/s
r (resistance per unit length)	8.4 ohms/m
c (capacitance per unit length)	48 pF/m
g (conductance per unit length)	49 μ S/m
l (inductance per unit length)	0.35 μ H/m
attenuation	0.44 dB/m

Once the coax was characterized the impact of varying the coax length was investigated using equation (1). In this case the array element impedance was used as Z_{load} . The transformed impedance across the expected passband of the device was analyzed for different lengths of coax above and below a quarter wavelength (2.0m) at the center frequency. A range of lengths were found where the phase angle within the passband reached zero degrees. The bandwidth was optimized by interpreting the band edges as the points where the phase angle fell to +/- 45°, a reasonable assumption when the phase angle passes through zero degrees. The results of this tuning are displayed in figure 1 below.

Figure 1 – Impedance and phase with and without coax for lensed element #1
Solid line is impedance, dotted line is phase



5. TRANSDUCER DESIGN AND FABRICATION

Three different array designs were fabricated and tested. The most recent design incorporated three ceramic “subelements” per element, an “air” kerf separating each element, a dual matching layer, and a TPX lens. The fabrication of this device is described below. Both one dimensional equivalent circuits and multi dimensional finite element models were used to analyze the design. The Redwood equivalent circuit in PSPICE was used to select matching and backing materials and provide

general design guidelines. For a more accurate representation of the performance the time domain finite element code PZFLEX (Weidleinger Associates, Inc, Los Altos, CA) was used.

A 2-2 composite was fabricated as described in section 2 and lapped to a thickness of 0.100mm. The ceramic posts were 0.025mm wide and the kerf was 0.008mm wide. Next, the conductive epoxy backing, acoustic impedance of 5.5 Mrayls, was cast in place on the back of the composite. This backing was lapped flat and a frame was bonded to the edges of the entire assembly. This frame was fabricated from a machinable ceramic with a low dielectric constant. It was used to provide a surface for the conductive traces connecting each element on the face of the array. Once this frame was in place an additional 0.047mm was lapped from the face, for a final composite thickness of .053mm.

Interconnect reliability was a significant problem with the first prototypes. Sputtered Au/Cr electrcodes were used to wrap the traces around the edges of the machinable ceramic. A dicing operation was then used to separate the wraparound traces. This method resulted in a loss of interconnect through small breaks in the metallization. An electroless deposition process proved more reliable, but adhesion was still problematic. Most recently posts of brass have been added to the machinable ceramic for conductivity in only the z-direction. Preliminary results are encouraging.

A conductive epoxy (5.9 Mrayl) was used as the first matching layer in order to decrease the possibility of losing electrical connection to one of the elements. A concern with this epoxy was the attenuation of 112 dB/mm at 30 MHz. This high value was probably due to the large silver flakes incorporated into the epoxy matrix. Since the desired matching layer thickness as determined from modeling was .014mm, a 3dB reduction in the sensitivity was expected. This attenuation, although undesirable, could be tolerated, and may even help to decrease near field clutter in the image [16].

After casting the first matching layer in place and lapping to thickness the elements were separated using a dicing saw and a 0.012mm blade. The depth and thickness of the kerf was critical. The depth of the kerf affected crosstalk and ringdown [14]. A larger kerf meant a smaller element size, reduced impedance, and an increased grating lobe amplitude in the focused beam. If a kerf filler was used such a wide kerf could also translate into lateral modes within the filler falling within the passband of the device.

As expected from the work of Dias [14], the depth of separation into the backing was found to be crucial. Finite element analysis was used to investigate this effect. Six different separation depths were modeled and the impulse response was inspected for amplitude and ringdown. A long "tail" on the waveform indicated a resonance within the backing due to the periodicity of the dicing. A higher than expected amplitude was a result of crosstalk. A separation depth of at least 18 μ m into the backing was needed to reduce the amplitude and ringdown to near the levels for a fully separated backing. Further modeling was performed using differential dicing, where kerf depth alternated between two values. Dicing 18 μ m and 36 μ m into the backing was found to provide the best result, a 64 % bandwidth and a ringdown of slightly more than two cycles. This model did not yet incorporate the TPX lens.

The element to element spacing was 0.099mm, or almost two wavelengths at the design center frequency. This would place grating lobes in the array at 30°. In order to determine the impact of the grating lobes the directivity pattern of the array was calculated. The directivity of each element was determined using the non-rigid baffle condition [13]. Discrete frequencies throughout the passband were analyzed as well as focusing throughout the depth of field. The worst case scenarios showed the grating lobes at -10dB relative to the main lobe for the one-way response. This would be unacceptable in most imaging systems. Broad bandwidth, however, may help to ameliorate this problem. If a pulsed response is considered, the 1-way amplitude is reduced by the ratio of the number of cycles in the pulse to the number of active channels [10]. For our array this reduction would be at least -12dB, considering a two cycle pulse and a simple 8 channel system. Additional channels would result in a greater reduction. Grating lobes should therefore be at a manageable level assuming a two cycle impulse response is achieved.

After separating the elements a second matching layer (3.1 Mrayls) was bonded to the face. A special bonding technique was developed so that adhesive would not flow into and fill the kerfs. This air kerf was used to reduce the element-to-element crosstalk within the array. The matching layer was prepared by lapping to 0.018mm thick and carefully waxing to a flat base. Shims, several microns thicker than the matching layers, were then placed adjacent to the layer. A high viscosity epoxy (Insulcast 501, American Safety, Roseland, NJ) was used as the adhesive. A thin, uniform film of the epoxy was scraped over the matching layer using the shims as a guide for a flat edged tool. The epoxy was cured slightly for 20 minutes to raise the viscosity and the array was pressed into place. Light pressure was applied and the assembly was cured. Analysis

of the kerf (using electron microscopy) and the bond line (using scanning acoustic microscopy) revealed uniform adhesion across the face and minimum infiltration of the epoxy into the kerf.

Addition of the TPX lens to the array proved very challenging. TPX, or Polymethylpentene, is a rigid plastic with low values of acoustic impedance (1.8 Mrayls at 30 MHz) and attenuation (6 dB/mm at 30 MHz) [11]. Chemically it is similar to Polypropylene and requires surface preparation before bonding. Two methods of preparation are Corona discharge and a Toluene based chemical adhesion promoter [15]. Experiments demonstrated that adhesion promoter 459T (Lord Chemical, Erie, PA), when applied to a clean TPX surface, resulted in dramatically enhanced adhesion. Epo-Tek 301 (Epoxy Technology, Billerica, MA) was then used to bond the TPX to the face of the second matching layer. The bond line between the TPX and the second matching layer was less than 1 μ m.

In order to provide proper alignment of the lens with the elevation aperture the lens was machined subsequent to bonding. A ball end mill was used in combination with an alignment fixture to mill the cylindrical curvature in the face. The depth of cut was controlled to within 0.005mm. After machining, a polishing operation was used to provide a mirror finish to the lens.

The connection of the coax to each element was achieved using a precision soldering station, low melting point Indium based solder, and a 50x microscope. In the future a flex circuit may be used to connect all the individual coaxes, but for the four element prototypes this simple method proved adequate.

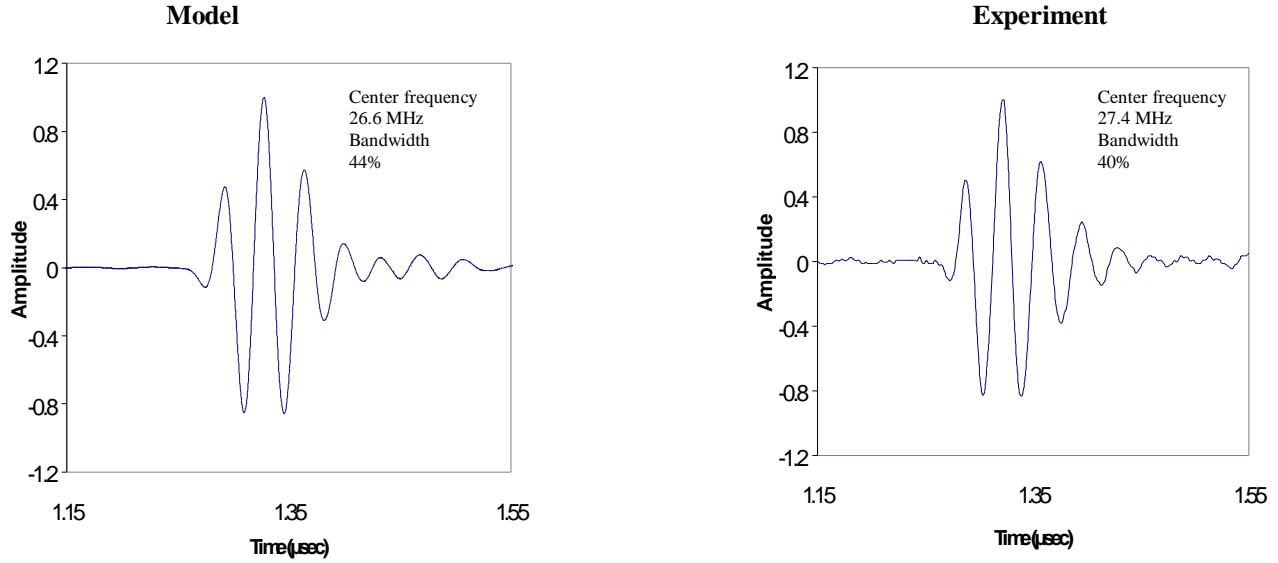
6. EXPERIMENTAL RESULTS

Three different prototype transducers, each with four active elements, were fabricated and tested. The first device incorporated a single matching layer and 0.066mm element-to-element spacing. The second device included a single matching layer and 0.099mm element-to-element spacing. Both of these prototypes were tested using a flat plate target at a distance of 1mm from the face of the device. The third prototype incorporated the dual matching layers and TPX lens described in section 5. The elements in this last device were tested using a flat plate target placed at the focal point.

The simplest design incorporated a single 3.3 Mrayl impedance matching layer and an element pitch of 0.066mm. This resulted in two ceramic subelements per element. A shallow isolation cut, 5 μ m deep and 17 μ m wide, was used to separate the elements. Most of the element-to-element separation was therefore provided by the composite filler. This epoxy filler was very hard and possessed minimal attenuation (9 dB/mm). Crosstalk was expected to be a problem for this design, but if the test results proved promising the fabrication process could be greatly simplified. Instead of dicing to provide element isolation a photolithographic process could be used on a plate of composite material.

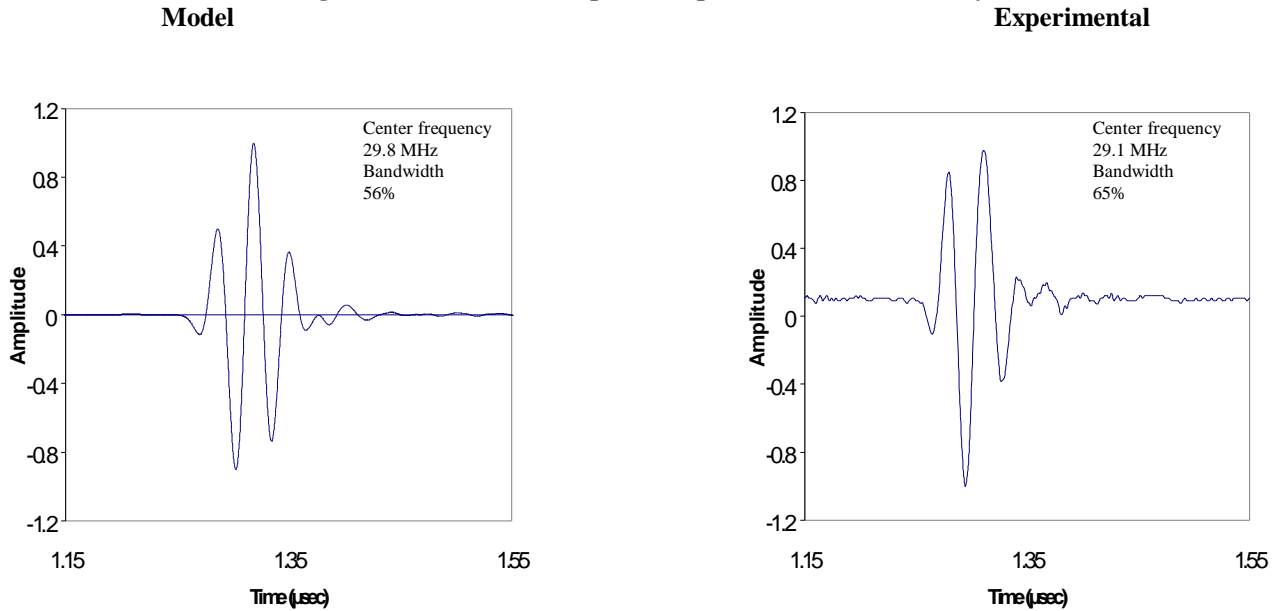
PZFLEX was found to be a powerful tool not only for predicting array performance but also for troubleshooting problems and determining design constraints. Issues such as the required depth of the isolation cut (between the major elements of the array), the required velocity and attenuation in the kerf filler, and the impact of bond lines were determined using this software. The finite element model for this first prototype predicted a maximum element-to-element crosstalk of -21dB, while the experimental results revealed -25dB of crosstalk. A comparison of the modeled and actual pulse echo impulse responses is shown in Figure 2. Of the four responses the one with the lowest bandwidth is displayed. The amplitudes of the responses were all within 15% of the average and the pulse shapes were similar. These first results displayed the utility of finite element modeling and demonstrated that 30 MHz arrays could be fabricated and tested.

Figure 2– Normalized Impulse Response, First Test Array



A second test array incorporating a single matching layer was also constructed. The element pitch was 2λ , with three ceramic subelements per element. This resulted in a larger element and a lower electrical impedance when compared to the 1.3λ spaced array. This lower impedance was more effectively transformed to 50 ohms using the coax and broader bandwidth resulted. Experimentally, the bandwidth was 65% and the pulse length was less than 2 cycles. Figure 3 displays the modeled and experimental impulse responses for this array. Although there is some disparity between the actual and modeled results, the agreement is still good. Slight deviations in actual materials values, such as a shift of $1\mu\text{m}$ in the matching layer thickness, may account for the deviation.

Figure 3 – Normalized Impulse Response, Second Test Array



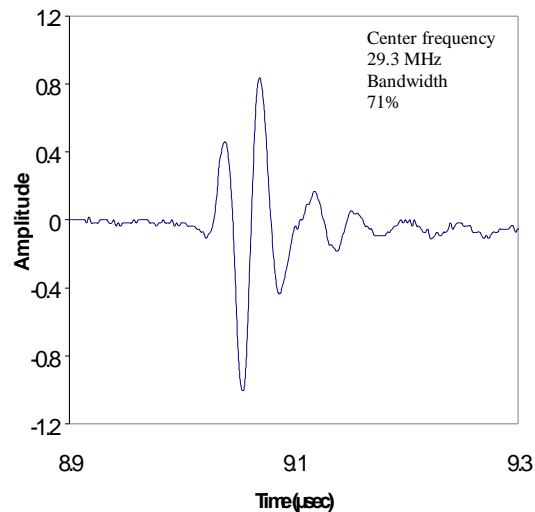
The third and final test array incorporated two matching layers and a TPX lens. The fabrication of the array was described in section 5. For this array a finite element model of the final design was not attempted. In order to account for the lens in the elevation direction a three-dimensional model, as opposed to the two-dimensional model used for the other arrays, was required. Modeling of the array without the lens was performed to ensure that the two matching layers provided a compact impulse response and that the array would focus properly. Without the lens the finite element model predicted a bandwidth of 64%. The TPX lens used a radius of curvature of 2.38mm for a predicted focal point of 7.7mm. Experimentally the focal point of the array was determined to be 7mm. The impulse response for element 1, tested at this focal depth, is displayed in Figure 4.

A problem with this third array was a loss of connection to the elements on one side. As a result crosstalk data was unavailable. A design change incorporating a more reliable interconnect method is being implemented to correct this problem.

7. SUMMARY

Methods for fabricating 2-2 composites and arrays for applications above 20 MHz have been developed. The composites possessed high coupling ($k_t > 0.65$) and lateral mode frequencies near 60 MHz. The arrays incorporated backing, matching, and elevational focusing. Coaxial cable was used for electrical impedance matching and an air kerf separated the elements. Finite element and one-dimensional modeling was used to analyze and refine the design. Experimental results show that 70% bandwidth can be achieved. Agreement between model and experiment was excellent.

**Figure 4 – Normalized Impulse Response, Third Test Array
Experimental**



8. FUTURE WORK AND ACKNOWLEDGEMENTS

A number of issues have been identified which need to be addressed before a fully sampled array is constructed. Several improved interconnect methods are being tested. A first matching layer material with a slightly higher impedance and lower attenuation is being investigated. Acceptable crosstalk levels will be verified experimentally and the directivity of individual

elements measured to insure proper array performance. Shielding will be added to the array between the lens and outer matching layer. Once these investigations are complete a 48 element array incorporating a flex circuit for interconnect will be fabricated.

The authors extend their appreciation to Gene Gerber for assembly of the arrays, Chiaki Miyasaka for acoustic microscopy, and Haifeng Wang for materials measurement. Additional acknowledgements are due to Jack Hughes, Geoff Lockwood, and David Vaughan at Weidlinger Associates. Financial support was provided through NIH grant P41-RR11795.

- [1] M. Lethiecq, et al., "Miniature High Frequency Array Transducers Based on New Fine Grain Ceramics," *1994 Ultrasonics Symposium*, 1994, pp.1009-1013.
- [2] A. Nguyen-Dinh et al., "High Frequency Piezo-Composite Transducer Array Designed for Ultrasound Scanning Applications," *1996 IEEE Ultrasonics Symposium*, 1996, pp. 943-947.
- [3] Y. Ito et al., "A 100 MHz Ultrasonic Transducer Array Using ZnO Thin Films," *IEEE Transactions on UFFC*, vol. 42, no. 2, pp. 316-324, March 1995.
- [4] P. A. Payne. et al., "Integrated Ultrasound Transducers," *1994 Ultrasonics Symposium*, 1994, pp.1523-1526.
- [5] M. O'Donnell and L.J. Thomas, "Efficient Synthetic Aperture Imaging from a Circular Aperture with Possible Applications to Catheter Based Imaging," *IEEE Transactions on UFFC*, vol. 39, no. 3, pp. 366-380, May 1992.
- [6] Endosonics Corporation Web Site (<http://www.endosonics.com>)
- [7] J. Stevenson et al., "Fabrication and Characterization of PZT/Thermoplastic Polymer Composites for High Frequency Phased Arrays," *J. Am. Ceramic Soc.*, 77[9], pp. 2481-2484, 1994.
- [8] X. Geng, "Numerical Modeling and Experimental Study of Piezocomposite Transducers", PhD thesis in Materials, Penn State University, December 1997.
- [9] W. J. Hughes. Personal Communication
- [10] A. Macovski, *Medical Imaging Systems*, N.J., Prentice Hall Inc., 1983.
- [11] T. Ritter, K.K Shung, X. Geng, H. Wang, and T.R. Shrout, "30 MHz Medical Imaging Arrays Incorporating 2-2 Composites," presented at *The 1998 IEEE Ultrasonics Symposium*, Sendai, Japan, October, 1998.
- [12] A. P. Albrecht, "Transmission Lines," *Electronic Designer's Handbook*, L.J. Giacoletto ed., N. Y., McGraw-Hill, pp. 8.1-8.78, 1977.
- [13] A. R Selfridge, "The Design and Fabrication of Ultrasonic Transducers and Transducer Arrays," PhD thesis in Electrical Engineering, Stanford University, July, 1982.
- [14] J.Fleming Dias, "An Experimental Investigation of the Cross Coupling Between Elements of an Acoustic Imaging Array Transducer," *Ultrasonic Imaging*, vol. 4, pp. 44-55, 1982.
- [15] Manny Mafilios, Matsui Plastics, Inc., personal communication
- [16] R. McKeighan, "Design Guidelines for Medical Ultrasonic Arrays," *Medical Imaging 1999: Ultrasonic Transducer Engineering*, vol. 3341, K. Kirk Shung editor, pp. 2-18, SPIE, Bellingham WA, 1998.